Development of a hydro-environmental model for inland navigational canals

Dongfang Liang, Rebecca W. Zeckoski and Xiaolin Wang

ABSTRACT

Before railroad and lorry traffic became common, many canals were built for transportation purposes. Water quality in canals has become a major concern as maintenance of these historically active canals has declined. A generic canal model has been developed to simulate the hydro-environmental processes specifically relevant to inland navigational canals, namely lockage, weir overflow, boat traffic, and algal growth. Apart from the movement of water, three types of particulate matter are tracked: algae (chlorophyll-a), inorganic non-cohesive sediment, and inorganic cohesive sediment. The newly developed model was applied to the Kennet and Avon Canal in southern England. The method of determining the input parameters for the model was documented herein, including setting up a Hydrological Simulation Program – Fortran model to obtain the landscape flow and sediment runoff to the canal. The model predictions were compared with the observed hydrological, sediment, and chlorophyll-a data at monitoring locations along the canal, and favourable agreements were achieved.

Key words | algal growth, canals, Kennet and Avon Canal, sediment transport, water quality

Dongfang Liang (corresponding author)
Department of Engineering Mechanics,
MOE Key Laboratory of Hydrodynamics,
Shanghai Jiao Tong University,
Shanghai 200240,
China
E-mail: *d.liang@sjtu.edu.cn*

Rebecca W. Zeckoski
Department of Engineering,
University of Cambridge,
Cambridge,
UK
(Now at Zeckoski Engineering,
Charlotte, NC 28202, USA)

Xiaolin Wang
Cardiff School of Engineering,
Cardiff University,
UK
(Now at Peterborough Office,
Halcrow Group Limited, UK)

INTRODUCTION

There are many canals and navigable waterways in the United Kingdom with the potential to contribute poor quality water to natural streams (Swanson *et al.* 2004). During their heyday, circa 1,840, nearly 6,600 km of inland waterways existed, including both canals and rivers that were made navigable (Hadfield 1981). Over the subsequent years, railroads and lorry traffic led to a decline in canal use. By the time of the 1968 Transport Act, when all existing canals in Britain were classified into commercial waterways, cruiseways (for amenity use only), and remainder waterways, only 3,220 km remained. Of these, 917 km were classified as 'remainder' waterways: not legally abandoned, but not financially maintained by the Government. For them, private groups, such as the Kennet and Avon Canal Trust, voluntarily contribute to the maintenance of the canals. Some of these historic canals have experienced poor water quality. Hence, private citizens and Government officials alike will benefit from computer models that can simulate the hydro-environmental processes in inland waterways in light of environmental concerns.

Although many hydrodynamic models exist for riverine systems, few canal models exist (Heatlie *et al.* 2007). In particular, while modelling efforts have been undertaken for irrigation and drainage canals (e.g., Sutcliffe & Parks 1987; Misra *et al.* 1991), there seems to be a dearth of research on canals used for navigation. Some well-known canals have been modelled, but the flow in them is driven differently from that in inland waterways. Coraci *et al.* (2007) developed a detailed model of the Venice canal network, where the flow is driven by the tidal action. Abril & Abdel-Aal (2000) studied the hydrodynamics of the Suez Canal, which is driven primarily by the sea level difference between the two ends of the canal. Heatlie *et al.* (2007) modelled the Manchester ship canal, but only from the flood risk management point of view.

Inland navigational canals may be replenished by natural rivers or pumping stations. They also receive surface

doi: 10.2166/hydro.2013.021

runoff from river catchments, and are governed by boat traffic and other anthropogenic factors. In order to navigate through uneven terrain in calm waters, canals essentially consist of a series of impoundments ('reaches') separated by locks (Willby *et al*. 2001). The lock structure maintains impoundment water levels while allowing boats to pass up or down sloped terrain. Lock gates are arranged in pairs spaced a standard distance apart, and the maximum acceptable boat size for a given canal is set by the lock dimensions on the canal. The reaches between the locks are often long; in a gently sloped landscape they may exceed 1.5 km. In a steep incline, however, they are short. The water surface in the reach is fairly flat and easily navigable, in contrast to the unnavigable natural stream in the same natural topography. A typical lock and part of a reach are shown in Figure 1.

The canal lock allows boats to move from one water elevation to another. The interior of a typical lock is shown in Figure 1(a), and the schematics of a typical lock structure are given in Figure 2. From the plan view, it is evident that each lock gate is made of two panels forming a convex angle against the direction of water movement. From the elevation view, it can be seen that past the upstream lock gate the bottom of the lock drops to the level of the downstream reach. This cill is evident in Figure 1(a) where a person is standing. A sluice is installed for each lock gate. As shown in Figure 2(b), the sluice for the upstream gate is located near the bottom of the canal sidewall; water can transit through this sluice and into the lock from an opening in the side of the lock wall. The downstream sluice labelled in Figure 2(b) is located near the bottom of the downstream gate to allow water to drain out of the lock when needed. As a boat moves through a lock, it is necessary to completely fill or drain the lock (as appropriate) so the water level on both sides of the gate to be opened is equal; otherwise the water pressure behind the gate is too great for individuals to push the gate open. Canal users open and close the sluice doors as they move through the lock from one elevation to the next. Before entering the lock, users open the sluice on the same side of the lock as their boat is currently located, leaving it open until the water level equalises, then close the sluice. After the boat enters the lock, the opposite sluice is opened and again the boaters wait until the water level in the lock equalises with that of their destination reach; finally the sluice is closed, the gate opened, and the boat moves on after closing the gate behind.

Figure 1 | Photos of a lock and reach on the Kennet and Avon Canal. (a) Interior of a typical lock, (b) part of a reach near the lock gate.

The hydraulic and water quality processes in canals differ from those in lakes or rivers. Rivers have a high flushing rate and lakes tend to be stagnant enough to act as settling basins; however, canals are somewhere in the middle, essentially made of a series of impoundments with intermediate retention time. Although canals have a much lower flow rate than rivers, the individual impoundments are not completely stagnant. Boat traffic dominates both the hydrodynamics and sediment generation and transport in canals. Boat passage increases the flow rate, as boats

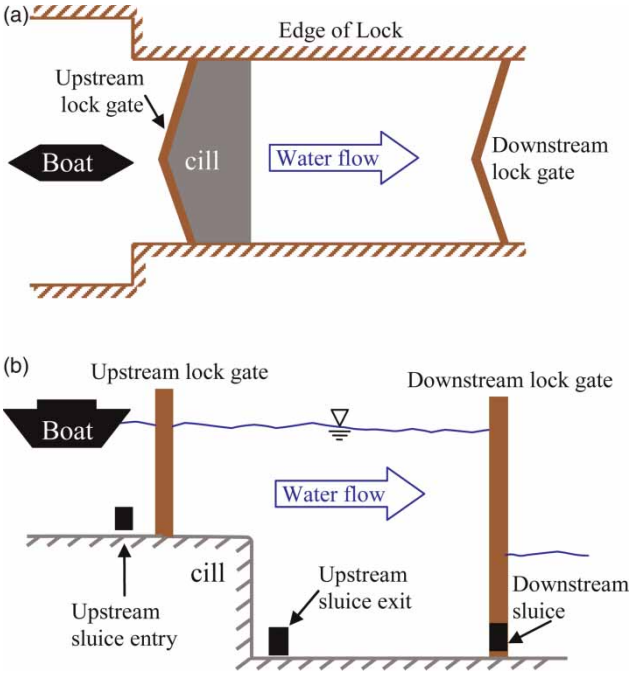

Figure 2 | Sketch of a lock. (a) Plan view, (b) elevation view.

remove large volumes of water from each reach as they pass through locks. The boats stir up noticeable quantities of bed sediment. To the authors' knowledge, there has not been a computer model designed for predicting the multiple hydro-environmental processes unique to inland navigational canals.

This study aims to develop a numerical model to evaluate the effect that canal operations have on water quality, specifically the concentrations of suspended particulates, including both inorganic sediment and biological materials. The reliability of the new canal model is verified in modelling the Kennet and Avon Canal in southern England, which has experienced severe water quality problems caused by high concentrations of inorganic sediment and algae (Neal *et al*. 2006a).

CANAL MODEL DEVELOPMENT

Overall method structure

The basic system simulated is a series of reaches connected by locks and weirs. In the canal model, each reach is naturally taken as a control volume, which has four basic state variables – water volume (V), cohesive sediment mass (S_{coh}), non-cohesive sediment mass (S_{non}), and algal mass (S_{alg}). The major variables of the solids are expressed as mass, rather than concentration, to simplify the present model framework. Knowing the water volume, mass and concentration can be easily converted from one to the other. Various inflows, outflows, sources and sinks associated with a reach can be represented as functions of these four variables. Based on the conservation of mass principle, a nonlinear ordinary differential equation can be written for each of the four quantities in a reach. The equations for all the reaches along a canal are coupled together, and can be solved numerically. Figure 3 lists all the relevant inflows and outflows that may be associated with a reach. They are all included in the developed model, for the sake of maintaining generality, whose detailed implementation can be found in Zeckoski (2010). However, some of them may be negligible for a specific canal. In the following subsections, only the key processes for the Kennet and Avon Canal are described.

It should be emphasised that the core model is a standalone receiving water model of the canal. Therefore, the processes less inherent to the canal operation, such as water/solids runoff, other external inputs, and abstractions, need to be supplied to the core model via time series generated outside the model. This increases the generality of the core model. The algorithms have been translated into computer code using the Microsoft Visual Basic 2008 programming language. A graphical user interface was created to aid the user in the input of needed parameters. In programming, objects were created to represent reaches and locks. It is hoped that the modularization of the code will make it easily portable for any future model developers who may take interest in it.

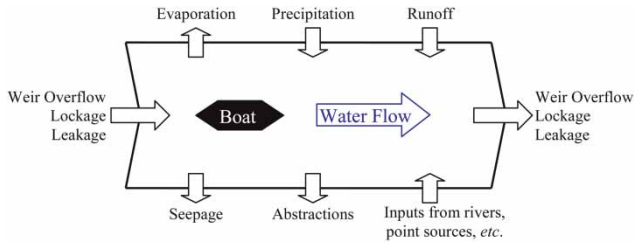

Figure 3 | Plan view of a reach and possible processes inside it.

Flow model

The water level along a canal is mainly controlled by three factors: one input control and two output controls. First, a relatively large and constant source of water feeds the summit reach of the canal; this may be pumped from a reservoir or may come from a natural feeding stream. This source water then trickles downstream to govern the water input to each successive reach. Insufficient input to the summit reach will cause the water depths in all reaches to drop. Excessive input to the summit reach may cause flooding. Given a sufficient input of water to the summit reach, the water level along the length of each reach is governed primarily by the height of the overflow weir, one of which can be seen in Figure 1(b). The overflow weirs are designed to carry all excess water above the desired depth to the next downstream reach. Thus, during normal steady-state operating conditions, the overflow weir determines the water level in the reach. The last major factor affecting the water level is boat traffic. The boat traffic directly affects water movement from one reach to the next. As boats move through the locks at the upstream and downstream end of each reach, the volume of water needed to fill and/or empty the lock is shifted from the upstream reach to the downstream reach. These three factors in a canal are designed to balance each other: the source of water is designed to be large enough to counteract the water loss through expected lockages, leakage, and seepage; and the overflow weirs allow water to bypass the locks while boats are absent.

The flow model quantifies these relationships unique to canals, including lock-associated flows (called lockages henceforth), weir flows, runoff, seepage losses, leakage, etc. Because the reaches between locks are designed to be level, flow due to the slope of the stream is insignificant, and thus a typical hydraulic model based on bed slope and roughness is inapplicable for these purposes. Equation (1) is the basic governing equation for the flow calculation in a reach:

$$\frac{dV}{dt} = Q_{\text{in}}(t) - Q_{\text{out}}(t) \tag{1}$$

where V is in m^3, t is time (s), $Q_{\text{in}}(t)$ represents the summation of the water inflow to the reach (m^3/s) as a function of time, and $Q_{\text{out}}(t)$ represents the summation of the water outflow from the reach (m^3/s) as a function of time. Only the mathematical representation of weir flow and lockages are elaborated herein, which are the two dominant processes in most cases. On canals used primarily for recreation, most of the boat traffic occurs in the tourist season in the summer. However, a certain amount of flow is supplied throughout the year to maintain the designed water level along the canal. Therefore, it is expected that lockages will dominate flow in the summer, while weir flows will dominate in the winter.

An overflow weir is typically positioned in the side wall near the downstream lock of a reach, shown in Figure 1(b). The weir normally discharges to the next lower canal reach, although occasionally a weir may bypass a reach or discharge into a neighbouring body of water, depending on the needs of the canal or the constraints of design the engineers considered during construction. The hydraulics of a canal weir is governed by basic weir flow and orifice flow equations. When the weir opening is not completely submerged, the flow rate above the weir is calculated from the contracted weir equation:

$$Q_{\text{weir}} = \frac{2}{3} C_{d,\text{weir}} (L_{\text{weir}} - 0.2H_{\text{weir}}) \sqrt{2g} H_{\text{weir}}^{1.5} \tag{2}$$

where $C_{d,\text{weir}}$ is the weir discharge coefficient (dimensionless, suggested to be 0.611 by Henderson (1966)), g is the acceleration due to gravity (m/s^2), L_{weir} is the length of weir crest (m), and H_{weir} is the depth of water above weir crest (m). Lateral contraction was noticed during the survey for the majority of the weirs along the canal, so the above unsuppressed weir equation is suitable. When the weir becomes submerged, the small entrance of the weir prevents the large weir conduit to be completely filled with water. In this case, Equation (3) for orifice flow is used:

$$Q_{\text{weir}} = \frac{2}{3} C_{d,\text{weir}} L_{\text{weir}} \sqrt{2g} \left[H_{\text{weir}}^{1.5} - (H_{\text{weir}} - H_{\text{sides}})^{1.5} \right] \tag{3}$$

where H_{sides} is the height of weir box opening (m). Equation (3), a modified form of the typical orifice equation, was presented by Daugherty (1937) and allows the smooth transition between weir and orifice flows needed for the numerical solution of the differential equations in the model. Q_{weir} is part

of the $Q_{out}(t)$ for the upstream reach, but is a component of $Q_{in}(t)$ for the downstream reach.

The total amount of water lost during boat passage through a lock depends on the state of the lock when a boat approaches it, which in turn is dependent on the direction of the previous boat compared to that of the current boat. Boats travelling upstream must enter a drained lock, and boats moving downstream must enter a full lock; likewise, boats moving upstream leave a full lock, and boats moving downstream leave a drained lock. Thus, if boats move in sequence, heading the same direction, each boat passage draws a full lock volume from the upstream reach and deposits a full lock volume in the downstream reach. If boats move through a lock in alternating directions, each boat passage will cause either a lock volume to be drawn from the upstream reach or a lock volume to be deposited in the downstream reach. It is evident that having boats move in alternate directions through a lock is an ideal situation, as it halves the amount of water needed compared to the same number of boats travelling in the same direction. However, it is difficult to force this in a real-world situation.

During boat passage through a lock, a volume of water equal to the volume of the lock will be taken from the upstream reach, or deposited to the downstream reach, or both. Equation (4) describes averaged flow rate considering these scenarios.

$$Q_{lock} = \left[(1 - E_{boat}) + \frac{E_{boat}}{2}\right] \cdot F_{boat} \cdot V_{lock} \quad (4)$$

where E_{boat} is the efficiency of boat movement defined as the ratio of the number of boats moving in opposite directions to the total number of boats (dimensionless), F_{boat} is the frequency of boat movement (boats/s), and V_{lock} is the volume of lock (m^3/boat). The term ($1–E_{boat}$) in Equation (4) represents the contribution by the boats moving through the lock sequentially in the same direction; the term $E_{boat}/2$ represents the contribution by the boats moving consecutively in opposite directions. An entire lock volume is lost from the reach every time a boat passes the lock going the same direction as the previous boat, but the same volume is lost only every other time a boat passes the lock going the opposite direction of the previous boat.

Water quality model

General

As mentioned before, the main water-quality parameters of concern in this study are suspended particulate matter. Hilton & Phillips (1982) investigated boat traffic effects on turbidity. They reported that suspended solids in trafficked waterways originated from both elevated phytoplankton levels and sediment generated by boat movements. The generation and transport of suspended solids in a canal can be considered a function of boat movements, the factors affecting algal growth, and the characteristics of inflow/outflow routes. Because the flow rate inside a canal reach is typically low, the flow velocity has negligible influence on the inorganic and organic solids distributions. With the exception of evaporative and seepage losses, solids exit a reach at all locations where water exits the reach. The concentration of solid particulates in an outflow depends on the position of the exit. In general, discharges that involve the whole water column can be assumed to hold solids at the average concentration of the reach, whereas discharges from the top of the water column hold a concentration different from the average value. In this paper, only the most important solids generation mechanisms are discussed.

The primary instigators of inorganic sediment flux in a reach are boat traffic and lockages. As a boat traverses the reach, its propellers stir up sediment from the bottom of the canal. Because inorganic sediment is heavier than water, its deposition in largely stagnant waters is an important feature. At the upstream end of a reach, significant turbulence accompanies the release of water from the upstream reach, whether the source is the weir overflow, leakage, or lockage. Hence, solids can be considered well-mixed at the upstream end of the reach. Towards the downstream end, water becomes quiescent and the inorganic sediment in the reach undergoes deposition.

Organic solids may include detritus from the land surface and faecal material, but free-floating algae (or phytoplankton) are of the greatest concern. Unlike other sources of organic material, algae are living and will reproduce in water. The low flow rate, and thus long residence time, in the canal encourages algal growth. The construction of canals eliminated trees close to water, and typical usage

patterns since their construction tend to keep the surrounding area clear, historically for horses to pass on towpaths, and more recently for walkers and bikers to use towpaths recreationally. As a result, light availability is typically high in a canal, which in turn leads to increased water temperature. All of these factors provide a beneficial habitat for algal growth, which can be an important contributor to solids concentrations when nutrients are available in sufficient quantities to support algal growth.

Inorganic sediment

Inorganic sediment is tracked in two classes: cohesive and non-cohesive. Equation (5) is the basic governing equation for the inorganic sediment calculation in a reach.

$$\frac{dS}{dt} = QS_{\text{in}}(t) - QS_{\text{out}}(t) - \frac{w_s S}{D} \tag{5}$$

where S represents the mass of either non-cohesive sediment (S_{non} in mg) or cohesive sediment (S_{coh} in mg), $QS_{\text{in}}(t)$ is the summation of the sediment inflow to the reach as a function of time (mg/s), $QS_{\text{out}}(t)$ is the summation of the sediment outflow from the concerned reach as a function of time (mg/s), w_s is the fall velocity (m/s), and D is the water depth. The only difference between the treatments of the non-cohesive and cohesive sediment is the calculation of the settling flux. The fall velocity of non-cohesive sediment is a straightforward function of the particle diameter (Soulsby 1997):

$$w_s = \frac{v}{d}\left(\sqrt{10.36^2 + 1.049D_*^3} - 10.36\right) \tag{6}$$

where v is the kinematic viscosity of water (m²/s), d is the diameter of sediment (m), and D_* is the dimensionless grain size defined as:

$$D_* = \left[\frac{g(s-1)}{v^2}\right]^{1/3} d \tag{7}$$

with s being the specific gravity of sediment (2.65 for fluvial sediment).

Due to their large surface area and charge, cohesive sediments have a tendency to flocculate, resulting in a larger fall velocity than that of individual particles. The empirical relationship developed by Manning (2004) has been adapted to estimate the mass settling flux, which is based on the cohesive sediment concentration and bed shear stress. A key feature of Manning's work is the separation of cohesive particles into 'macroflocs' (flocs with diameter >160 μm) and 'microflocs' (flocs with diameter <160 μm), whose relative contributions to the total mass settling flux depend on the ratio of the suspended macroflocs to suspended microflocs, r_{sed}:

$$r_{\text{sed}} = 0.815 + 3.18 \cdot 10^{-6} \cdot \frac{S_{\text{coh}}}{V} - 1.4 \cdot 10^{-10} \cdot \left(\frac{S_{\text{coh}}}{V}\right)^2 \tag{8}$$

With a near-zero flow velocity and thus bed shear stress, the fall velocities of macroflocs ($w_{s,\text{macro}}$) and microflocs ($w_{s,\text{macro}}$) are:

$$w_{s,\text{macro}} = 6.44 \cdot 10^{-4} + 4.71 \cdot 10^{-10} \cdot \frac{S_{\text{coh}}}{V} \tag{9}$$

$$w_{s,\text{micro}} = 2.44 \cdot 10^{-4} \tag{10}$$

The total mass settling flux is then:

$$w_s \cdot S_{\text{coh}} = \left[\left(1 - \frac{1}{1+r_{\text{sed}}}\right) \cdot \left(S_{\text{coh}} \cdot w_{s,\text{macro}}\right)\right] + \left[\frac{1}{1+r_{\text{sed}}}\left(S_{\text{coh}} \cdot w_{s,\text{micro}}\right)\right] \tag{11}$$

In a typical canal, it is expected that the boat contributions to the inorganic sediment greatly exceed those from weir flow, runoff and external sources. The boat travelling generates a plume of sediment in the wake. As the boat traverses a reach, it will cause sediment production along the entire length of the reach, and thus the concentration stirred up by the boat is multiplied by the volume of the disturbed water to obtain the total sediment load generated by the boat in the reach. Bird's-eye views of the boats cruising on the Kennet and Avon Canal were found in Bing.com (Microsoft Corporation), which clearly show that the width of the boat-generated plume is approximately equal to the boat width. It is assumed that the sediment load is

evenly distributed from the bottom of the canal to the water surface, roughly in a rectangular cross-section. An estimate of the boat-disturbed sediment concentration can be made by on-site sampling. Then, the total mass of sediment generated by a boat in a reach is:

$$QS_{\text{boat}} = F_{\text{reach}} \cdot S_{\text{boat}} \cdot L \cdot D \cdot W_{\text{boat}} \tag{12}$$

where F_{reach} is the frequency of boat passage in the reach (boats/s), which may differ from the boat passage frequency at locks F_{boat} in Equation (4), if there is a winding hole where boats might turn around or a mooring area where they may stop for an extended time and thus not transit the full reach; S_{boat} is the field-surveyed suspended sediment concentration generated by boat propellers (mg/m^3); L is the reach length (m); and W_{boat} is the boat width taken to be equal to the width of the sediment plume (m).

In addition to the inorganic sediment sink/source due to deposition and boat traffic, sediment input/output may take place in association with water inflow/outflow. Weir outflows are a major year-round water route, but the weir crest is often just a few centimetres below the water surface, compared to the canal depth of approximately 1.5 m. Hence, most inorganic sediment should have settled out of the top water layer by the time it reaches the overflow weir near the downstream end of a reach, resulting in minimal sediment flux through the weir. This sediment flux is calculated in the model as a function of the sediment remaining in the water above the weir crest, i.e., the sediment that has not deposited below the weir crest after moving through the reach according to Equations (6) and (11), with the detailed algorithm given in Zeckoski (2010). By contrast, the lockage-induced sediment transfer between neighbouring reaches can be significant. A large slug of sediment is expected to move from one reach to the next with each lockage, because the water used to fill the lock is drawn from near the bottom of the reach. Furthermore, this movement happens in direct association with the sediment disturbance caused by the opening of the lock gates and boat manoeuvres. Therefore, the sediment that moves with water to fill the lock and subsequently discharge downstream is assumed fully mixed. Hence, it is assumed that sediment transfer between canal reaches via lockages happens at the average concentration of the reach, giving:

$$QS_{\text{lock}} = Q_{\text{lock}} \cdot \frac{S}{V} \tag{13}$$

Apart from this bulk movement of sediment with the flow, Zeckoski (2010) also considered the sediment generation by the movement of lock doors during the lockage, but subsequent analyses showed that the influence of this process was not significant. This paper focuses on the most important influencing factors, thus omits the sediment increase from the lock doors scraping the bottom.

Algal model

Research has shown that live algae attempt to keep themselves suspended in the euphotic depth (e.g. Malone 1980). The algal death and the resulting settling are not considered separately, but are incorporated indirectly as part of the growth rate. The mass conservation of algae needs to include both algal growth and hydrologic transport (e.g. Pridmore & McBride 1984). The basic model equation for algae is given as Equation (14):

$$\frac{dS_{\text{alg}}}{dt} = QS_{\text{alg,in}}(t) - QS_{\text{alg,out}}(t) + \mu \cdot S_{\text{alg}} \tag{14}$$

where S_{alg} is the algal biomass as mentioned before (mg), $QS_{\text{alg,in}}(t)$ is the summation of the algal inflow to the reach as a function of time (mg/s), $QS_{\text{alg,out}}(t)$ is the summation of the algal outflow from the concerned reach as a function of time (mg/s), and μ is the algal growth rate (s^{-1}). As can be seen later, the algal growth rate will be negative if there is insufficient nutrient to support the existing algal population.

In keeping with the primary factors found in the literature, temperature, light availability, and nutrient level are regarded to most affect algal growth. A maximum growth rate is first calculated based on water temperature, and is then modified to take into account other controlling factors. Given ample light and nutrients, the maximum growth rate as restricted by water temperature can be written as (Eppley 1972):

$$\mu_{\max,T} = \frac{\ln 2}{86400} \cdot 0.851 \cdot 1.066^{T} \tag{15}$$

where $\mu_{\max,T}$ is the maximum growth rate (s^{-1}) at water temperature T (°C). This maximum growth rate for algae in the canal is then limited by light availability as described by Bicknell *et al.* (2001):

$$\mu_{\max} = \mu_{\max,T} \cdot \frac{LI}{K_{s,l} + LI} \tag{16}$$

where $\mu_{\max}$ is the maximum growth rate based only on temperature and light availability (s^{-1}), LI is the light intensity (J/m^2s), and $K_{s,l}$ is the Michaelis-Menten constant for light-limited growth (set at 23.012 J/m^2s based on the recommendation of Dugdale & MacIsaac 1971).

The limiting nutrient for algal growth is defined by the relative abundance of different types of nutrients. The algae in a body of water typically consist of a multitude of species. Although they have slightly different chemical compositions, it has been found that their chemical makeup, in terms of carbon (C), nitrogen (N), and phosphorus (P), is generally uniform ($C_{106}N_{16}P$) (e.g. Søballe & Threlkeld 1985). Data from Neal *et al.* (2006a) indicate that the algal growth is P-limited in many inland canals. For the Kennet and Avon Canal, the average N : P weight ratio is 28.8, yielding an N : P molar ratio of 63.7. This is much greater than the 'ideal' molar ratio of 20 given by Cooper (1937) and the P-limited ratio of 12 given by Dillon & Rigler (1974). Therefore, the growth rate is limited according to phosphorus availability based on the equation developed by Pridmore & McBride (1984), and can be expressed in model terms as:

$$\mu = \mu_{\max} \cdot \frac{r_{\text{chl}} \cdot S_P^{1.178}/2.449 - S_{\text{alg}}/V_{\text{ED}}}{r_{\text{chl}} \cdot S_P^{1.178}/2.449} \tag{17}$$

where r_{chl} is the conversion ratio from chlorophyll-a mass to dry algal biomass taken to be 60 herein, S_P is the total phosphorus concentration (mg/m^3), and V_{ED} is the euphotic volume of the reach. The value of 60 for r_{chl} was chosen after a survey of literature estimated values ranging from 6.7 to 1,861 with an average value of 107 and a median value of 65; Zeckoski (2010) provides the detailed survey. Algae are dynamic creatures, so it is not surprising to find a wide range of r_{chl}. Algae are considered be present from the water surface to the depth that light penetrates.

$$V_{\text{ED}} = \begin{cases} V & \text{if ED} \geq D \\ L \cdot W_{\text{reach}} \cdot \text{ED} & \text{if ED} < D \end{cases} \tag{18}$$

where W_{reach} is the width of the reach, and ED is the euphotic depth defined as the depth of light penetration. Following Bicknell *et al.* (2001), ED can be calculated by:

$$\text{ED} = \frac{4.60517}{\text{LITALG} \cdot S_{\text{alg}}/V_{\text{ED}} + \text{LITSED} \cdot (S_{\text{non}} + S_{\text{coh}})/V + \text{EXTB}} \tag{19}$$

where LITALG is the light extinction coefficient due to algae, LITSED is the light extinction coefficient due to inorganic sediment, and EXTB is the base light extinction coefficient. They are taken to be 0.0012 $m^2\,mg^{-1}$, 0.000025 $m^2\,mg^{-1}$ and 1.67 m^{-1}, respectively, in reference to Van Duin *et al.* (2001).

Algae move from reach to reach largely following the same paths as water. The suspended algae may temporarily move outside the euphotic zone and still be productive, so algae may actually be found beyond the euphotic depth, with the exact distribution depending on the mixing property of the flow. Lacking information on the mixing depth and the algae distribution in the considered canal reaches, this study simply assumes that algae are uniformly distributed over the euphotic depth and ignores their possible presence elsewhere and the nonuniformity in their distribution. The weir overflow may transport a significant amount of algae, as weirs draw water from the light-saturated portion of the reach. The corresponding algal flux is a product of the concentration of algae in the euphotic volume and the flow rate through the weir.

$$QS_{\text{alg,weir}} = Q_{\text{weir}} \cdot \frac{S_{\text{alg}}}{V_{\text{ED}}} \tag{20}$$

Conversely, the turbulence associated with the lockage operation implies that the algae entering and leaving a lock will be thoroughly mixed in the lockage water. Therefore, lockages may be regarded to draw water from the entire water column, and the associated

algal flux is:

$$QS_{\text{alg,lock}} = Q_{\text{lock}} \cdot \frac{S_{\text{alg}}}{V} \tag{21}$$

Solution algorithm

Due to the existence of some highly nonlinear terms, Equations (1), (5) and (14) have no analytical solution. The present canal model uses an implicit central Euler scheme to solve these differential equations numerically. Taking the hydraulic Equation (1) for example, it can be discretised into:

$$V^{n+1} = V^n + \frac{(Q_{\text{in}}^n - Q_{\text{out}}^n) + (Q_{\text{in}}^{n+1} - Q_{\text{out}}^{n+1})}{2} \cdot \Delta t \tag{22}$$

where the superscripts n and $n+1$ designate the consecutive two time levels, and Δt is the time step (s). The computation is carried out sequentially from upstream reaches to downstream reaches in each time step. In this way, the components of the inflow are known at each time step, but most of the outflow components are dependent upon the storage. Hence, Equation (22) and its equivalents for sediment and algae are nonlinear algebraic equations. Newton's Method was chosen to simultaneously seek their solutions iteratively. Complete details on the solution of the system of equations are provided in Zeckoski (2010).

MODEL APPLICATION

General

The Kennet and Avon Canal was chosen as the site to demonstrate the use and reliability of the new canal model, predominantly due to the tense political climate around the canal and the resulting need for a computer model capable of predicting solids loads. The canal eventually discharges into the visually pristine River Kennet, creating water quality problems. By personal communication with various individuals while attending the users' meetings of the canal and river, the authors learnt that the Environment Agency is considering numerous management options to address the water quality problem caused by the canal, so it is desirable to have a model capable of predicting the outcomes of these options before committing funds to any restoration efforts. In addition, numerous groups have made available varied spatial water-quality data to the authors, creating an ideal setting for the testing of the new canal model.

Relevant to this application, Zeckoski (2010) had successfully verified the model by simulating the hydro-environmental processes of a hypothetical canal system in extreme scenarios and conducted sensitivity analyses on key parameters to identify the influence that those parameters have on various aspects of model output. The model had been found to behave properly under all conditions. The following subsections present the modelling procedures and results concerning the practical application of the model. Because the simulation is over several years, the catchment runoff contribution to the canal flow and sediment concentration should be taken into account. For this purpose, a separate overland model has been established.

Overland model

Runoff from the land surface has the potential to enter the canal, and there are areas where the canal interacts with the nearby rivers, so it is important to understand the nature of the drainage area surrounding the canal and the rivers. The water and sediment runoff and river inputs are assumed to occur independently of the flow and water quality in the canal. They should be provided as external time series of values to the core canal model. Figure 4 shows the River Kennet and its tributaries. As shown in Figure 4(a), the canal parallels the natural course of the River Dun to the south and west of Hungerford. After the Dun joins the Kennet, the canal parallels the River Kennet to the east of Hungerford. Two major surface streams contribute flow to the canal: Froxfield Stream deposits approximately a quarter of its flow into the canal through a control structure (the remainder flows in a culvert underneath the canal to join the Dun), and Shalbourne Brook contributes all of its flow to the canal, though a large portion of it is removed via a weir on the opposite side of its entry point on the canal; the removed

(a)

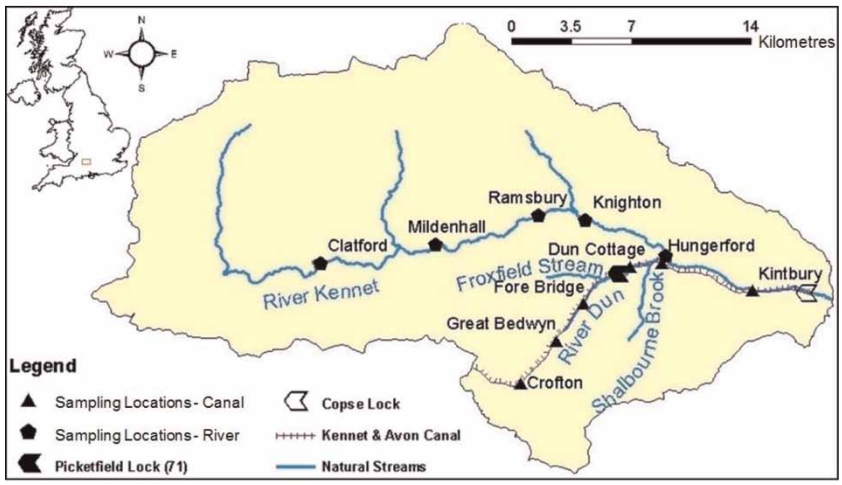

(b)

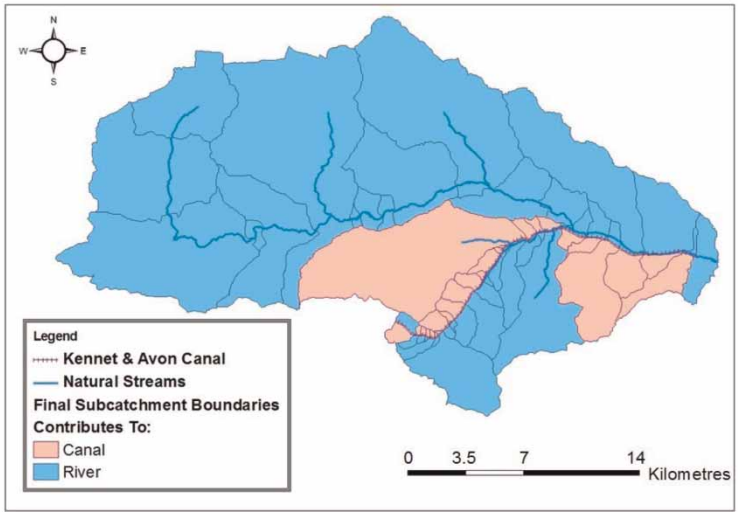

Figure 4 | The Kennet and Avon Canal and the Kennet Catchment. (a) Locations of the catchment and relevant sites, (b) subcatchment delineation.

water continues along the natural flow path of Shalbourne Brook (National Rivers Authority 1992). Additionally, small amounts of water are drawn at various points from the River Dun and the River Kennet and deposited in the canal (National Rivers Authority 1992; Halcrow Group Limited 2007). The Hydrological Simulation Program – Fortran (HSPF) was chosen to set up a separate catchment model for the River Kennet and the Kennet and Avon Canal. It is possible to use other catchment models to generate necessary inputs to the canal model.

This area is predominantly agricultural, with a loamy soil texture, roughly 30% sand, 45% silt, and 25% clay (Jarvis *et al.* 1979). The digital elevation model originally generated by the Centre for Ecology and Hydrology was used to divide the whole catchment into subcatchments. Some intermediate subcatchments were split along the watershed between the rivers and the canal. The final catchments were then classified as contributing to the canal or contributing to the rivers depending on whether they fell on the canal side or the river side. In doing this, it was

assumed that any area between the canal and the river contributed to the river, as the canal bank was typically slightly elevated above the river bank. Some very small subcatchments have been carefully created along the canal, whose borders coincide with the locks to establish a one-to-one correspondence between the subcatchments and the canal reaches. Therefore, the correct runoff could be apportioned to each reach of the canal. The segmentation of rivers also takes into account the locations of the river gauges.

After delineation, the overland model was successfully calibrated and verified against the monitored flows and sediment concentrations on the river provided by the Environment Agency. Because the overland model is not the focus of this paper, the detailed results are not presented herein, but can be found in Zeckoski *et al*. (2009) and Zeckoski (2010). In coordination with the application of the canal model, the runoff and sediment transported from the land surface and diverted from the rivers were exported from HSPF to text files for all the subcatchments linked to the canal reaches. Each text file contained the total volume of flow and mass of inorganic sediment delivered to each reach of the canal.

Canal model setup

The studied area covers 21 km of the Kennet and Avon Canal and consists of 26 locks, from the Crofton Top Lock (lock number 55 in Figure 5) eastward to Copse Lock (downstream of Kintbury labelled in Figure 4 and corresponding to lock number 80 in Figure 5), where the canal merges with the River Kennet. Correspondingly, there are 25 reaches between the locks, plus a summit reach upstream of the Crofton Top Lock, making a total of 26 reaches. The shortest reaches on this section of the Kennet and Avon Canal are in the steep flight of locks approaching the summit reach on the west, where the canal ascends approximately 12 m through eight locks over the space of approximately 2 km. The longest reach in the studied area on the Kennet and Avon Canal is just over 1.5 km long. The reach widths of the canal range from 7.4 to 13.3 m. It should be noted that the water levels shown in Figure 5 are only rough estimates according to the positions of the weir crests, as they are slightly higher in the winter, with no lockage demands, and are slightly lower in the boating season in the summer. The heights of overflow weir crests above the bottom of the canal range from 1.10 to 1.53 m. On-site sampling by the authors in 2009 shows that the average lock width is 5.2 m, the average lock volume is 205 m^3, and the overflow weir dimensions vary greatly, but are generally several metres long.

British Waterways provided information on the lockage rates and limited flow data recorded on the canal (Langridge 2004). An annual count of the total lockages is available at several locks. A representative weekly distribution of lockages based on data compiled from multiple canals in England was also available, shown in Figure 6. From these data, the frequency of boat movement F_{boat} can be estimated and distributed to all the locks based on proximity to the monitored locks. The lockages follow a seasonal trend of being high in the summer and low in the winter. Visual inspections by the authors on the canal suggest that the efficiency of lockage use E_{boat} is close to 0.67.

Total phosphorus concentration was calculated on a monthly basis from data collected at the Centre for Ecology

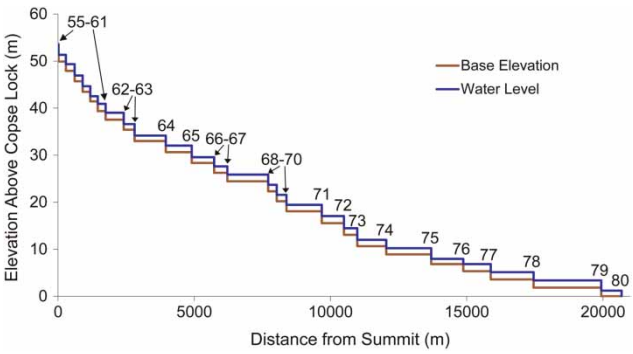

Figure 5 | Bed elevations, water levels and lock numbers of the study canal.

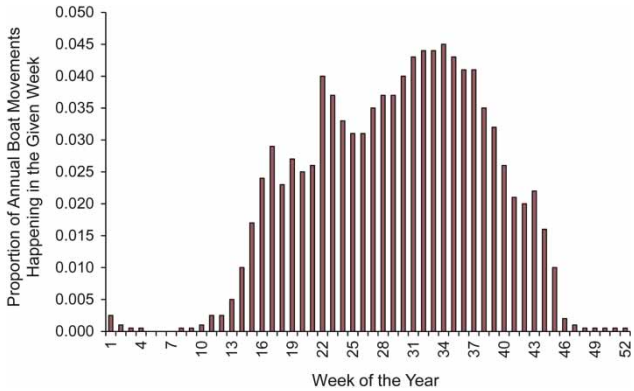

Figure 6 | Weekly distribution of lockages in a year.

and Hydrology (Neal *et al.* 2006a) at 10 stations in the region. The phosphorus concentration in each reach on the canal was estimated using data from the closest observation station. Measured water temperatures in the Kennet and Avon Canal range from 1.5 to 22.7 °C, but the daily variation of the water temperature is not available. Hence, as suggested by Beer (2001), the daily-averaged temperature is assumed to change sinusoidally during a year:

$$T = T_{\text{mean}} + T_{\text{mag}} * \sin\left(\frac{2\pi t_d}{365} + T_{\text{phase}}\right) \tag{23}$$

where T_{mean} is the mean annual temperature (12 °C), T_{mag} is the magnitude of the annual temperature variation (6.54 °C), T_{phase} is the phase parameter (4.46 radians), and t_d is the Julian day. It is seen from Figure 7 that this sinusoidal curve provides a good fit to data collected by Neal *et al.* (2006a).

The majority of the flow in the top 16 impoundments of the studied reach is supplied via the summit reach, to which the Crofton Pumping Station pumps water at a variable rate year-round. The water pumped at Crofton is drawn from nearby Wilton Water, a manmade reservoir designed for this purpose. There is a constant 'baseflow' pumped year-round to compensate for leakage, seepage, and evaporative losses, which was first estimated as 125 L/s based on private communication with the Crofton Pumping Station. Additionally, an extra flow rate is pumped in the summer boating season to compensate for lockages; the initial estimate of this flow rate with the most confidence is 80 L/s. Sediment and phosphorus levels in the feed water were

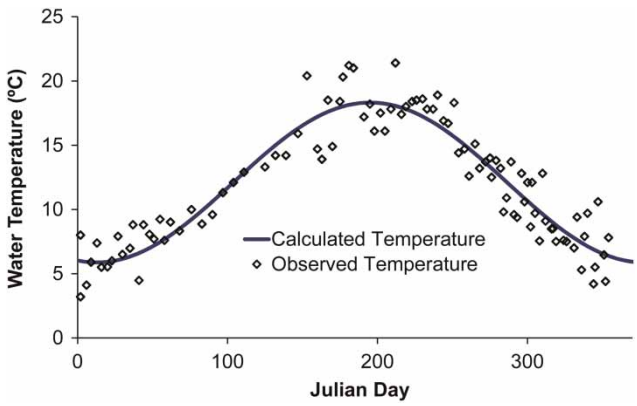

Figure 7 | Sinusoidal fit to the observed water temperatures on the canal.

estimated according to Neal *et al.* (2006a). Solar radiation can be estimated from the latitude (51°24′N) and cloud cover of the studied area according to the relation developed by Hamon *et al.* (1954) and implemented by the WDMUtil program (Hummel *et al.* 2001). Cloud cover was calculated from the hours of sunshine available at the MetOffice website (www.metoffice.gov.uk).

Non-cohesive particle diameter was set to 0.2 mm, which is the mid-range value given by Jarvis *et al.* (1979). In order to determine the amount of sediment disturbed by boat movement, water samples were collected immediately before and after boat passage in two field surveys by the authors. Through laboratory analyses, the median concentration of the sediment stirred up by boat passage was approximately 13.5 mg/L, allocated to non-cohesive (4.5 mg/L) and cohesive (9.0 mg/L) forms according to an area-weighted average soil texture in the catchment as determined from Jarvis *et al.* (1979).

To start the time-marching procedure, initial conditions need to be specified. Because the water level in a canal is held mostly constant by design, the initial water storage V of each reach is calculated by assuming that the water is at the overflow weir level. The initial storage of inorganic sediment can be specified at zero, corresponding to the situation with no boat traffic. The initial storage of algae in the reach is calculated as half that supportable by the monitored phosphorus level, given abundant light. Experimentation with the model showed that the effects of initial conditions vanished within a month into the simulation, suggesting that, with a sufficient 'start up' time for the model, any inaccuracies generated by these simplistic estimates on initial conditions will disappear. The time step for the canal model was set to one day, which matches the resolution of the available input data.

Modelling results

A sensitivity analysis of the various input parameters was conducted. Zeckoski (2010) presents a full analysis of the sensitivity of the model to each input parameter. In summary, the total flow rate in the canal is most sensitive to the external flows that feed the canal; the flow through the weirs (used in calibration) is sensitive to multiple parameters but particularly the external inflows, the depth of the weir,

and the rate of abstractions from the reach. The sediment concentration was most sensitive to the frequency of boat movements and the sediment generated by boats. The algal concentration was most sensitive to the flow rate, temperature, external input of algae, and the light extinction coefficient. Most parameters used in the model are physically based, i.e., they can be measured. In the calibration description that follows, some physical parameters were adjusted because their initial estimation contained large uncertainty.

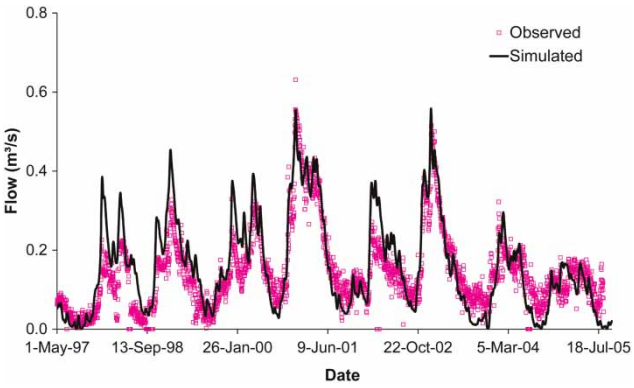

Figure 8 | Simulated and observed flows at Picketfield Lock (Lock 71).

Measured flow data are available on the canal over a weir that bypasses Picketfield Lock (Lock 71), which have been used to calibrate the canal model to the Kennet and Avon system. The comparison of observed and simulated bypass weir flows around Lock 71 is presented in Figure 8. It is evident that there is generally a good agreement between the observed and simulated flows, particularly in the years when good lockage data are available in 2000–2004. The errors in the average flow rates and median flow rates are 10% and 9%, respectively. This calibration was obtained through minimal alteration of the initial

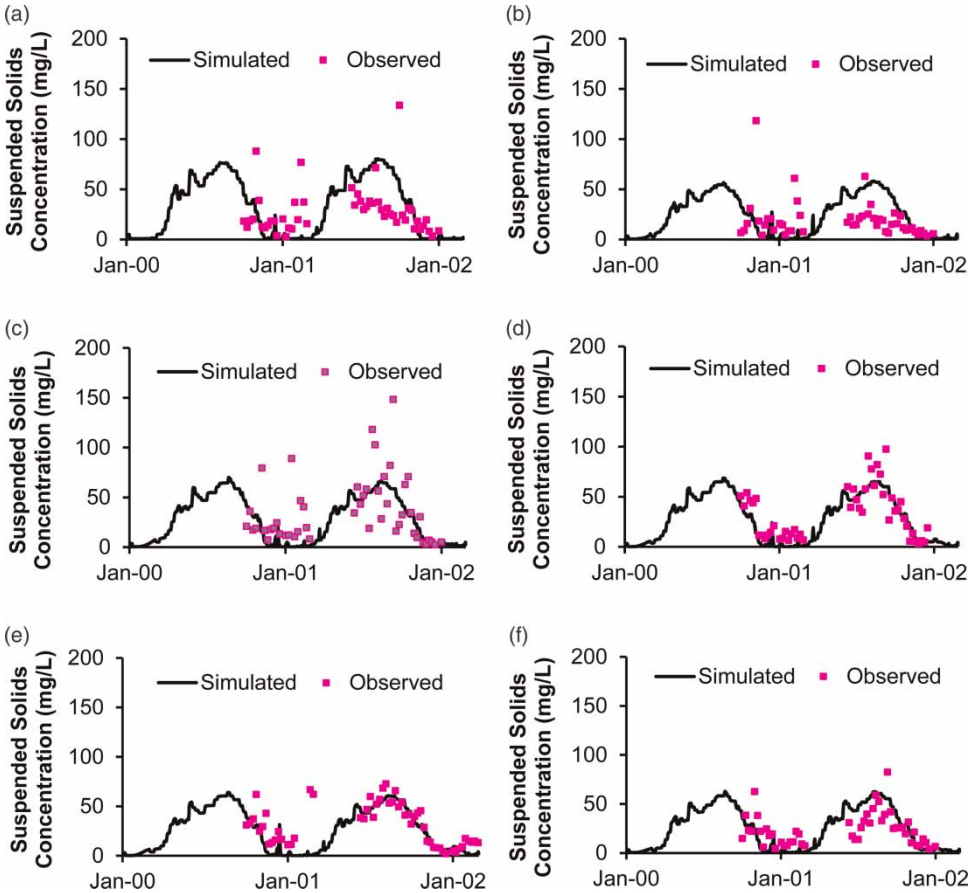

Figure 9 | Simulated and observed concentrations of the total suspended solids. (a) Crofton, (b) Great Bedwyn, (c) Fore Bridge, (d) Dun Cottage, (e) Hungerford, (f) Kintbury.

estimated parameters; the parameters adjusted were those with the most uncertainty: the inflow to the summit reach and the seepage rates through the sides of the canal. Both were adjusted within the range of values reported by experts and the literature.

Total solids data were available at six sites on the canal (Figure 4(a)), collected by the Centre for Ecology and Hydrology (Neal *et al.* 2006b). It was assumed that the observed data were representative of the average concentration of solid particulates in the reach. The observed data did not differentiate between organic and inorganic solids; thus the observed data were compared to total simulated solids concentrations (non-cohesive sediment, cohesive sediment, and algal dry mass) in the canal at these stations. The model agreement is further demonstrated in Figure 9. After calibration, the errors between the average simulated values in a 5-day window surrounding each observed data point (see Kim *et al.* (2007) for description of process) and the value of the observed data at that data point fell between ±30% for all stations; more detailed calibration statistics are provided in Zeckoski (2010). This calibration was achieved by adjusting the sediment disturbed by boats and the number of boats to associate with each lockage. Both parameters were adjusted within the range of data observed on the canal. The over-prediction of the suspended solids at the two uppermost stations, Crofton and Great Bedwyn between Jan 2001 and Jan 2002 might be attributed to the crude estimation of the flow rate and solids concentration at the Crofton Pumping Station. The effect of this boundary condition is weakened further downstream, so the agreement between the prediction and measurement is better at other stations.

Chlorophyll-a data, considered to be representative of algal concentration, were available at two sites on the canal (Crofton and Hungerford labelled in Figure 4(a)), again collected by the Centre for Ecology and Hydrology (Neal *et al.* 2005). Because the model predicts algal dry mass rather than chlorophyll-a concentration, the conversion factor r_{chl} used in Equation (17) was applied to the algal mass output to enable the comparison. As this chlorophyll-a to algal mass ratio varies with a multitude of conditions, and as algae are living organisms, considerable scatter is expected. However, it is seen from Figure 10 that

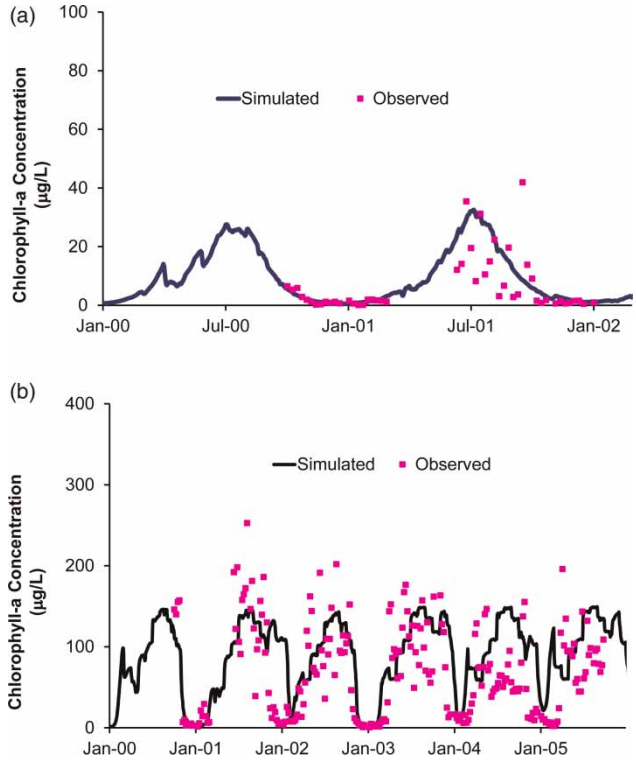

Figure 10 | Simulated and observed algal concentrations. (a) Crofton, (b) Hungerford.

the simulated values do reproduce the overall trend of the observed data. It seems that the uncertainty in r_{chl} can be at least partly compensated by the valuation of other parameters in the algal kinetics. After calibration, the errors between the average simulated values in a 5-day window surrounding each observed data point (see Kim *et al.* 2007 for description of process) and the value of the observed data at that data point fell between ±50% for all stations; more detailed calibration statistics are provided in Zeckoski (2010). The primary factor adjusted during the algal calibration was the base light extinction coefficient.

It is seen from Figures 9 and 10 that the annual patterns of the solids and algal concentrations experience similar seasonal changes. During the boating season in the late spring to early autumn, inorganic sediment concentrations will greatly increase compared to winter values. Algal growth in the summer far exceeds its growth in the winter due to increased water temperature and solar radiation in the summer. The gradual increases in temperature, sunlight, and boat traffic in the spring cause corresponding increases in solids concentrations, eventually peaking in mid-summer

and then falling off again gradually in the autumn. The model generally simulated these trends.

The application of this model in the future could be enhanced if more comprehensive data on flow, source water algal concentration, seepage rates, daily boat traffic, sediment disturbed by boat traffic, algal biomass, and external inflows/outflows were collected and used during the calibration process.

CONCLUSIONS

The development and testing of a new canal model have been presented in this paper. This canal model is able to quantify the effect that canal operations have on water quality. The governing equations for the flow, sediment transport and algal growth processes have been established. The hydraulic and water quality interactions between the canal and the natural landscape can be included by coupling the canal model with an external hydrological model. Solution algorithms have been developed and coded according to the finite difference method and Newton's iteration algorithm.

The newly developed model has been tested on the Kennet and Avon Canal. A catchment model, HSPF, was parameterized and used to determine the interactions between the canal and the natural landscape. Extensive data about the canal were drawn from readily available literature, existing agency databases, communication with stakeholders and field surveys. The effectiveness of the new canal model has been demonstrated in satisfactorily predicting the trends of flow, inorganic sediment transport and algal concentration in the canal.

The model developed herein is sufficiently general to allow its application to other canals. The value of the model will be further demonstrated in a following paper to examine and optimise the Kennet and Avon Canal management plans to improve water quality.

ACKNOWLEDGEMENTS

The digital elevation model was provided by Dr Andrew Wade. Some monitored water-quality datasets were provided by Dr Colin Neal. The first author appreciates the support of the Open Research Fund Program of the State Key Laboratory of Water Resources and Hydropower Engineering Science, Wuhan University (Grant No. 2011A005). The authors are also grateful to the anonymous reviewers for their constructive suggestions.

REFERENCES

Abril, J. M. & Abdel-Aal, M. M. 2000 A modelling study on hydrodynamics and pollutant dispersion in the Suez Canal. *Ecological Modelling* **128**, 1–17.

Beer, W. N. 2001 Six parameter water temperature model. Retrieved 3 September, 2009 from www.cbr.washington.edu/data/Streams.

Bicknell, B. R., Imhoff, J. C., Kittle Jr., J. L., Jobes, T. H. & Donigian Jr., A. S. 2001 *Hydrological Simulation Program - Fortran: HSPF, Version 12 User's Manual*. AQUA TERRA Consultants, Mountain View, California.

Cooper, L. H. N. 1937 On the ratio of nitrogen to phosphorus in the sea. *Journal of the Marine Biological Association* **22**, 177–182.

Coraci, E., Umgiesser, G. & Zonta, R. 2007 Hydrodynamic and sediment transport modelling in the canals of Venice (Italy). *Estuarine, Coastal, and Shelf Science* **75**, 250–260.

Daugherty, R. L. 1937 *Hydraulics: A Text on Practical Fluid Mechanics*. McGraw-Hill, London, 460 pp.

Dillon, P. J. & Rigler, F. H. 1974 The phosphorus-chlorophyll relationship in lakes. *Limnology and Oceanography* **19** (5), 767–773.

Dugdale, R. C. & MacIsaac, J. J. 1971 A computation model for the uptake of nitrate in the Peru upwelling region. *Investigatión Pesquera* **35** (1), 299–308.

Eppley, R. W. 1972 Temperature and phytoplankton growth in the sea. *Fishery Bulletin* **70** (4), 1063–1085.

Hadfield, C. 1981 *The Canal Age*. David and Charles, London, 233 pp.

Halcrow Group Limited 2007 *Kennet Chalkstream Restoration Project: Kennet Canal/River Scoping Final Report*. pp. 98.

Hamon, R. W., Weiss, L. L. & Wilson, W. T. 1954 Insolation as an empirical function of daily sunshine duration. *Monthly Weather Review* **82** (6), 141–146.

Heatlie, F., Drake, J. & Debski, D. 2007 Modelling the Manchester ship canal. *Water and Environment Journal* **21**, 100–107.

Henderson, F. M. 1966 *Open Channel Flow*. Collier-Macmillan Ltd, London, 522 pp.

Hilton, J. & Phillips, G. L. 1982 The effect of boat activity on turbidity in a shallow broadland river. *The Journal of Applied Ecology* **19** (1), 143–150.

Hummel, P., Kittle Jr., J. L. & Gray, M. 2001 *WDMUtil Version 2.0: A Tool for Managing Watershed Modeling Time-Series Data:*

User's Manual. AQUA TERRA Consultants, Decatur, Georgia, 165 pp.

Jarvis, M. G., Hazelden, J. & Mackney, D. 1979 *Soils of Berkshire*. Rothamsted Experimental Station, Lawes Agricultural Trust, Harpenden, 263 pp.

Kim, S. M., Benham, B. L., Brannan, K. M., Zeckoski, R. W. & Yagow, G. R. 2007b Water quality calibration criteria for bacteria TMDL development. *Applied Engineering in Agriculture* **23** (2), 171–176.

Langridge, J. 2004 Kennet & Avon Canal Sustainability Monitoring Report 2003–2004. British Waterways, 90 pp.

Malone, T. C. 1980 Algal size. In: *The Physiological Ecology of Phytoplankton* (I. Morris ed.). Blackwell Scientific Publications, Oxford, pp. 433–463.

Manning, A. J. 2004 *The development of new algorithms to parameterise the mass settling flux of flocculated estuarine sediments*. Report TR145, HR Wallingford.

Misra, R., Sridharan, K. & Kumar, M. S. M. 1991 Transients in canal network. *Journal of Irrigation and Drainage Engineering* **118** (5), 690–707.

National Rivers Authority, Thames Region 1992 *Kennet and Avon Canal: Survey of Interaction with the River Kennet*. National Rivers Authority, Thames Region, 27 pp.

Neal, C., House, W. A., Jarvie, H. P., Neal, M., Hill, L. & Wickham, H. 2005 Phosphorus concentrations in the River Dun, the Kennet and Avon Canal and the River Kennet, southern England. *Science of the Total Environment* **344** (1–3), 107–128.

Neal, C., House, W. A., Jarritt, N. P., Neal, M., Hill, L. & Wickham, H. 2006a The water quality of the River Dun and the Kennet and Avon Canal. *Journal of Hydrology* **330**, 155–170.

Neal, C., Neal, M., Leeks, G. J. L., Old, G., Hill, L. & Wickham, H. 2006b Suspended sediment and particulate phosphorus in surface waters of the upper Thames Basin, UK. *Journal of Hydrology* **330**, 142–154.

Pridmore, R. D. & McBride, G. B. 1984 Prediction of Chlorophyll a concentrations in impoundments of short hydraulic retention time. *Journal of Environmental Management* **19** (4), 343–350.

Søballe, D. M. & Threlkeld, S. T. 1985 Advection, phytoplankton biomass, and nutrient transformations in a rapidly flushed impoundment. *Archiv für Hydrobiologie* **105** (2), 187–203.

Soulsby, R. 1997 *Dynamics of Marine Sands: A Manual for Practical Application*. Thomas Telford, London, pp. 249.

Sutcliffe, J. V. & Parks, Y. P. 1987 Hydrological modelling of the Sudd and Jonglei Canal. *Hydrological Sciences Journal* **32** (2), 143–159.

Swanson, L. A., Lunn, R. J. & Wallis, S. G. 2004 Management of canal systems under the water framework directive: determining fundamental properties governing water quality. *Hydrology: Science and Practice for the 21st Century* **II**, 160–167.

Van Duin, E. H. S., Blom, G., Los, F. J., Maffione, R., Zimmerman, R., Cerco, C. F., Dortch, M. & Best, E. P. H. 2001 Modeling underwater light climate in relation to sedimentation, resuspension, water quality and autotrophic growth. *Hydrobiologia* **444**, 25–42.

Willby, N. J., Pygott, J. R. & Eaton, J. W. 2001 Inter-relationships between standing crop, biodiversity and trait attributes of hydrophytic vegetation in artificial waterways. *Freshwater Biology* **46**, 883–902.

Zeckoski, R. W. 2010 Water Quality Modeling for the Kennet and Avon Canal, a Navigational Canal in an Inland Catchment. PhD thesis, University of Cambridge, 230 pp.

Zeckoski, R. W., Lazar, A. N., Liang, D. & Wade, A. J. 2009 Comparison of the HSPF and HBV-INCA Models: Crossing the Atlantic Divide. *American Society of Agricultural and Biological Engineers Annual International Meeting*, Reno, Paper No. 096591, pp. 4474–4482.

First received 30 January 2013; accepted in revised form 9 August 2013. Available online 9 October 2013